Article

Cell Reports

Intrinsic Projections of Layer Vb Neurons to Layers Va, III, and II in the Lateral and Medial Entorhinal Cortex of the Rat

Graphical Abstract

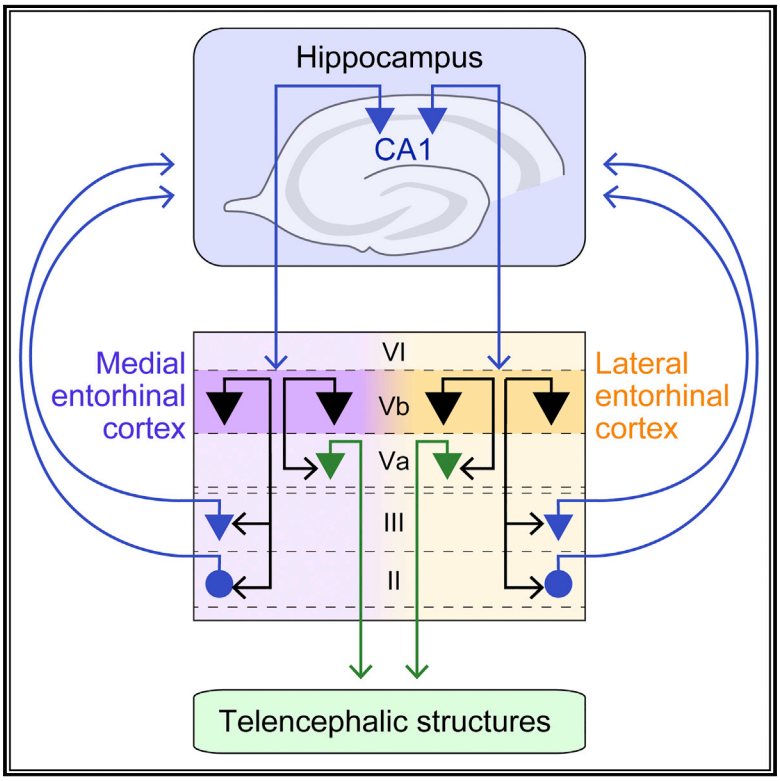

Authors

Shinya Ohara, Mariko Onodera, Øyvind W. Simonsen, ..., Toshio Iijima, Ken-Ichiro Tsutsui, Menno P. Witter

Correspondence

menno.witter@ntnu.no

In Brief

Ohara et al. demonstrate the intrinsic connectivity of layer Vb neurons of both the medial and lateral entorhinal cortex. Layer Vb neurons are key elements of two circuits in the hippocampus-memory system: a hippocampal-output circuit and a feedback loop to the hippocampus.

Highlights

- Layer V (LV) circuitry in lateral and medial entorhinal cortex is similar
- LV comprises two sublayers, Va and Vb, with Vb neurons projecting locally
- LVb neurons contact telencephalic projecting neurons in LVa
- LVb neurons also contact hippocampus-projecting neurons in LII and LIII

Ohara et al., 2018, Cell Reports *24*, 107–116
July 3, 2018
https://doi.org/10.1016/j.celrep.2018.06.014

CellPress

Cell Reports
Article

Intrinsic Projections of Layer Vb Neurons to Layers Va, III, and II in the Lateral and Medial Entorhinal Cortex of the Rat

Shinya Ohara,[1,2,5] Mariko Onodera,[1,5] Øyvind W. Simonsen,[2] Rintaro Yoshino,[1] Hiroyuki Hioki,[3,4] Toshio Iijima,[1] Ken-Ichiro Tsutsui,[1,6] and Menno P. Witter[2,6,7,*]

[1]Division of Systems Neuroscience, Tohoku University Graduate School of Life Sciences, Sendai 980-8577, Japan
[2]Kavli institute for Systems Neuroscience, Center for Computational Neuroscience, Egil and Pauline Braathen and Fred Kavli Center for Cortical Microcircuits, NTNU Norwegian University of Science and Technology, 7489 Trondheim, Norway
[3]Department of Morphological Brain Science, Graduate School of Medicine, Kyoto University, Kyoto 606-8501, Japan
[4]Department of Cell Biology and Neuroscience, Juntendo University Graduate School of Medicine, Tokyo 113-8421, Japan
[5]These authors contributed equally
[6]Senior author
[7]Lead Contact
*Correspondence: menno.witter@ntnu.no
https://doi.org/10.1016/j.celrep.2018.06.014

SUMMARY

Layer V of the entorhinal cortex (EC) receives input from the hippocampus and originates main entorhinal outputs. The deep-sublayer Vb, immunopositive for the transcription factor Ctip2, is thought to be the main recipient of hippocampal projections, whereas the superficial-sublayer LVa, immunonegative for Ctip2, originates the main outputs of EC. This disrupts the proposed role of EC as mediating hippocampal-cortical interactions. With the use of specific (trans)synaptic tracing approaches, we report that, in medial entorhinal cortex, layer Vb neurons innervate neurons in layers Va, II, and III. A similar circuitry exists in the lateral entorhinal cortex. We conclude that EC-layer Vb neurons mediate two circuits in the hippocampus-memory system: (1) a hippocampal output circuit to telencephalic areas by projecting to layer Va and (2) a feedback projection, sending information back to the EC-hippocampal loop via neurons in layers II and III.

INTRODUCTION

The entorhinal cortex (EC) constitutes the major gateway between the hippocampus and the neocortex and, together with the hippocampus, plays a critical role in memory and spatial navigation. Previous anatomical studies have shown that connectivity patterns of the superficial layers (layers I–III) and the deep layers (layers V and VI) of EC are strikingly different (Cappaert et al., 2015). The superficial EC neurons are the main though not exclusive recipients of cortical inputs, either directly or through adjacent cortices, and provide inputs to all subfields of the hippocampus via the perforant pathway. On the other hand, deep layer V (LV) neurons receive a substantial part of the hippocampal output via projections arising in field CA1 and the subiculum. This hippocampal output circuit via LV is considered to play an important role in transferring transiently stored information in the hippocampus to downstream neocortical networks for long-term memory formation (Buzsáki, 1996; Eichenbaum et al., 2012; Knierim, 2015). Entorhinal LV neurons also project to the superficial layers (Dolorfo and Amaral, 1998; Köhler, 1986, 1988; van Haeften et al., 2003), and it has been shown that the hippocampal information may re-enter the entorhinal-hippocampal loop (Iijima et al., 1996; Kloosterman et al., 2003a). This re-entrant activity (reverberation) is one of the mechanisms proposed for temporal storage of information in a neuronal network (Edelman, 1989; Iijima et al., 1996; Kloosterman et al., 2003a). Alternatively, these deep to superficial inputs would allow superficial neurons to compare incoming entorhinal information with hippocampally processed information (Buzsáki, 1996). This circuitry is assumed to be present in both the medial (MEC) and lateral subdivision (LEC) of the entorhinal cortex.

LV in rodents is commonly subdivided into two sublayers, layers Va (LVa) and Vb (LVb). The superficial LVa, adjacent to layer IV (lamina dissecans), comprises mainly large pyramidal neurons that are unequally distributed along the extent of both MEC and LEC. Cells in LVb appear smaller, more uniform in soma size and are more densely packed than their counterparts in LVa (Insausti et al., 1997). Recent studies in the mouse showed that these two sublayers in MEC can also be differentiated with respect to the expression patterns of transcription factors and their main connectivity (Ramsden et al., 2015; Sürmeli et al., 2015). Whereas LVa neurons express E twenty-six (ETS) variant 1 (Etv1), LVb neurons express chicken ovalbumin upstream promoter transcription factor (COUP-TF) interacting protein 2 (Ctip2). Regarding the connectivity, the latter authors showed that hippocampal afferents from CA1 terminate preferentially in LVb of MEC, whereas the efferent projections to telencephalic domains preferentially originate in LVa. This thus puts an additional synapse between neurons in LVb and LVa to close the postulated output circuit from the hippocampus to the neocortex. Neurons in LV are known to originate long-range and local intrinsic projections (Dolorfo and Amaral, 1998; van Haeften et al., 2003; Witter et al., 1989). Therefore, Sürmeli et al. (2015) hypothesized that neurons in LVb might

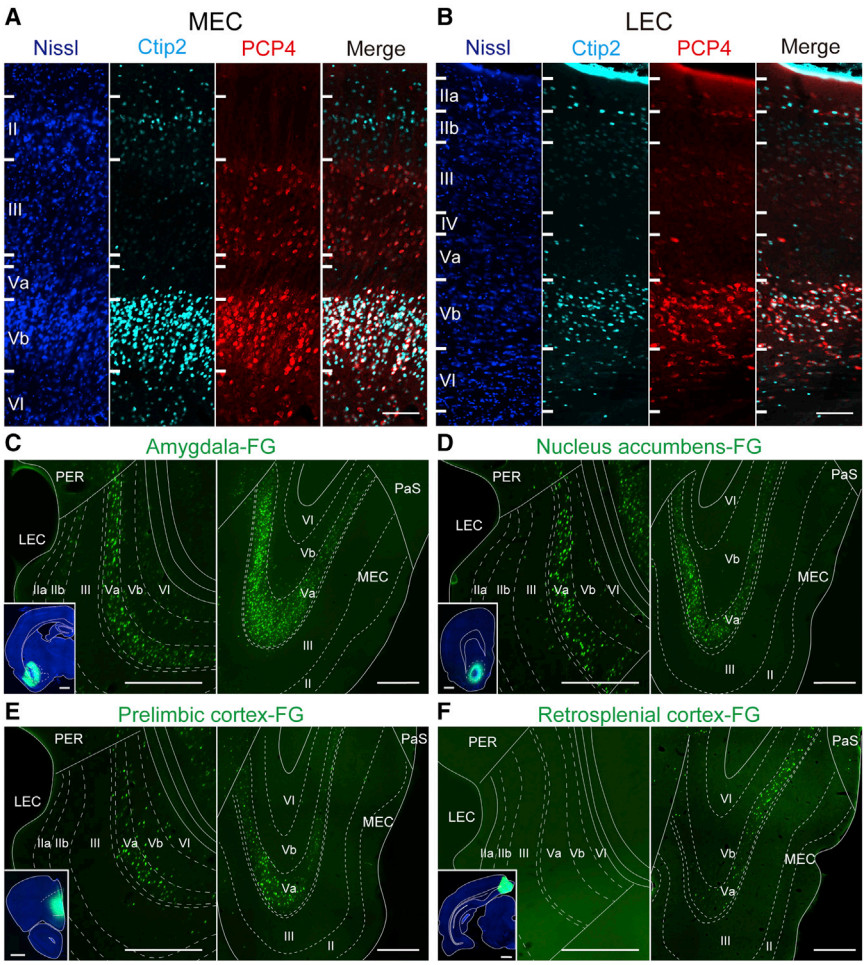

Figure 1. Differences in Molecular Identity and Telencephalic Projections between LVa and LVb in LEC and MEC

(A and B) Distribution of Ctip2- (cyan) and PCP4- (red) positive neurons in layer V in MEC (A) and LEC (B) is restricted to neurons in LVb. Note additional weaker and sparser labeling of neurons in layer II (Ctip2) and layer III (PCP4). Sections are counterstained with NeuroTrace (NTG, blue). Roman numbers indicate entorhinal layers.

(C–F) Retrograde labeling in LEC and MEC, resulting from Fluoro-Gold (FG) injections either into amygdala (C), nucleus accumbens (D), prelimbic cortex (E), or retrosplenial cortex (F), is restricted to LVa. Each coronal section shows retrograde labeling in LEC (left) and MEC (right). Inset shows the injection site of FG (green) in a section counterstained with NTG (blue).

The scale bars represent 100 μm for (A) and (B), 1,000 μm for the injection sites, and 500 μm for main panels of (C)–(F). Entorhinal layers in all subsequent figures are indicated with dashed lines and roman numbers. LEC, lateral entorhinal cortex; MEC, medial entorhinal cortex; PaS, parasubiculum; PER, perirhinal cortex.

contact neurons in LVa. However, proof of such a synaptic connection from neurons in LVb to neurons in LVa is currently lacking.

We further do not know whether a similar connectional differentiation between LVa and LVb exists in LEC. This might be hypothesized in view of convincing data that the population of pyramidal neurons in LV of LEC and MEC are morphologically and electrophysiologically indistinguishable and that also in LEC, LV originates the main entorhinal efferents to telencephalic areas (Canto et al., 2008; Hamam et al., 2000, 2002; Insausti et al., 1997).

In this study, we therefore aimed to identify the projection targets of LVb neurons in MEC and LEC. We opted to carry out these analyses in the rat, because this rodent species is still commonly used as an experimental animal in neuroscience. We first examined whether LV in LEC and MEC can be subdivided into LVa and LVb based on differential protein expression. To this end, we used immunolabeling to assess the distribution of Ctip2 and Purkinje cell protein 4 (PCP4) in EC and confirmed that LV in both LEC and MEC of the rat can be divided into Ctip2/PCP4-positive LVb and Ctip2/PCP4-negative LVa. With the use of anterograde tracing, we established in the rat that CA1 inputs specifically target LVb in LEC and MEC, similar to what was reported for MEC in mice. We also detailed the laminar distribution of some additional inputs to LV. We then examined the telencephalic projections of LV neurons by retrograde tracing, confirmed that telencephalic projections originate from LVa, but not LVb, in MEC, and showed that this scheme also applies to LEC. Most importantly, with the use of a transsynaptic retrograde tracing approach with rabies virus, we show that LVb neurons of LEC and MEC likely target both telencephalic-projecting LVa neurons and the hippocampus-projecting neurons in LII and LIII. We thus conclude that LVb neurons are the key elements of two main circuits in the hippocampus-memory system: a hippocampal output circuit to telencephalic areas by projecting to neurons in LVa and a feedback loop by projecting to neurons in LII and LIII.

RESULTS

In Both LEC and MEC, LVa and LVb Differ with Respect to Molecular Identity and Projections

To examine whether the EC LV of the rat can be further divided into two sublayers, we examined the distribution of Ctip2- and PCP4-positive neurons in both MEC and LEC (Figures 1A and 1B). In line with the previous mouse study, Ctip2- and PCP4-positive neurons distributed densely in MEC LVb (Kitamura et al., 2017; Sürmeli et al., 2015). Ctip2-positive neurons were also observed in MEC LII, and PCP4-positive neurons were observed in MEC LIII, which is in line with a previous study (Figure 1A; Tang et al., 2015).

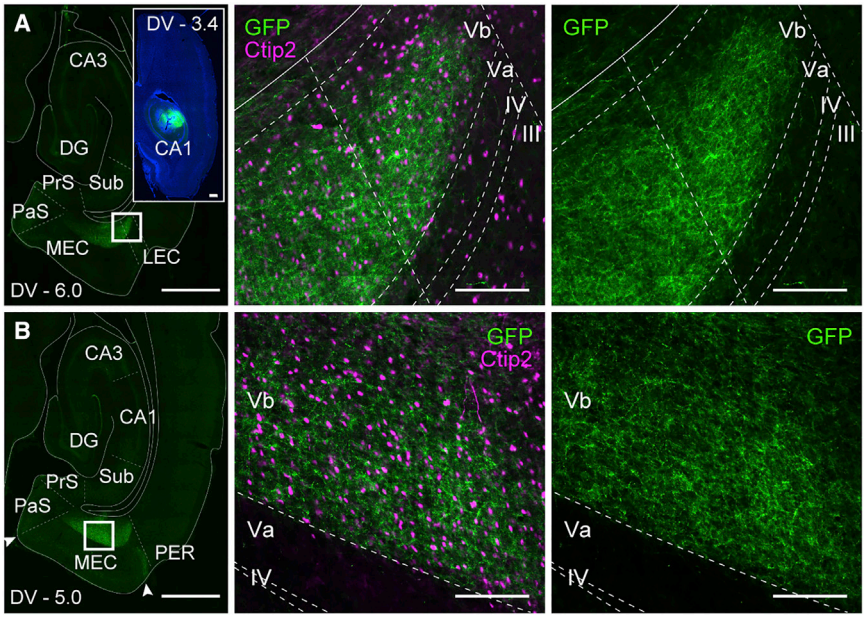

Figure 2. Terminal Distribution of Hippocampal Inputs to LVa and LVb in LEC and MEC.

Selective distribution of anterogradely GFP-labeled fibers in LVb in LEC (A) and MEC (B) following Tet-off lentiviral vector injection into CA1. Inset shows the injection site in section counterstained by NTG (blue). The middle and right-hand panels represent the boxed areas in LEC and MEC with and without staining for the transcription factor Ctip2, marking neurons in LVb (magenta). The scale bars represent 1,000 μm for the low-magnification images and 100 μm for the high-magnification images.

In LEC, Ctip2- and PCP4-positive neurons were preferentially and densely present in the deeper portion of LV (Figure 1B), similar to MEC. In both MEC and LEC, the Ctip2- and PCP4-immunopositive neurons in LVb mainly had a small cell soma, and the overall distribution and density of these labeled neurons was similar in both EC divisions. As for the other layers in LEC, Ctip2-positive neurons were seen in superficial portion of LII (LIIa) as well. In contrast to MEC, PCP4-labeled neurons were not prominent in LIII. Our data thus indicate that not only in MEC but also in LEC in the rat, LV can be divided into two sublayers by a layer-specific gene expression pattern, similar to what was reported for the mouse MEC (Sürmeli et al., 2015).

In the latter study, it was further reported that LVa and LVb in mouse MEC differ with respect to their main efferent projections such that telencephalic projections originate mainly from LVa neurons, but not from LVb neurons. To test whether this is true in the rat and whether LV in LEC shows a similar organization, we conducted a series of retrograde tracing experiments with a focus on main telencephalic targets of projections from MEC and LEC (Insausti et al., 1997; Agster and Burwell, 2009). Retrogradely transported chemical tracers were injected into either the basolateral amygdala (BLA) (n = 2), nucleus accumbens (NAc) (n = 2), prelimbic cortex (PrL) (n = 2), or the retrosplenial cortex (RSC) (n = 2). Injections into the BLA, NAc, and PrL resulted in numerous labeled neurons in LVa of both LEC and MEC. In case of RSC injections, labeled neurons were observed in MEC LVa, but not in LEC. In all cases, retrogradely labeled neurons were rarely observed in LVb of either LEC or MEC (Figures 1C–1F). These results thus show that main telencephalic projections originate preferentially from LVa neurons, but not from LVb neurons, in both LEC and MEC. These results in the rat are thus in line with and extend the observations in mouse MEC (Sürmeli et al., 2015).

Our data did not confirm the presence of a sparse population of neurons in LVb giving rise to long-range projections to the anterior thalamus (Sürmeli et al., 2015). Injections of retrogradely transported chemical tracers either into the anteromedial or laterodorsal thalamic nuclei did not result in labeled neurons in any layer of LEC or MEC (Figure S1). This is not due to a failure of transport of the tracers as many retrogradely labeled neurons were observed in the deep layers of presubiculum (PrS) and parasubiculum (PaS), in line with previous studies (Sürmeli et al., 2015; Vertes et al., 2015). Our results thus indicate that, in the rat, in contrast to the mouse but in line with previous rat studies (Kerr et al., 2007), neurons in LVb of both LEC and MEC do not project to the anterior thalamus.

LVa and LVb Differ with Respect to Inputs

Layer V of EC is considered as the main recipient of hippocampal projections originating in CA1 and subiculum (Kloosterman et al., 2003b; Köhler, 1985a; van Haeften et al., 2003). Additional inputs arise from the medial septal complex (MS) and medial prefrontal and retrosplenial cortex (Alonso and Köhler, 1984; Czajkowski et al., 2013; Fuchs et al., 2016; Hasselmo, 2013; Jones and Witter, 2007; Sugar et al., 2011). In none of these studies, a separation between LVa and LVb has been made, and it is only in a recent paper in mice that it is reported that CA1 project almost exclusively to LVb of MEC (Sürmeli et al., 2015). We therefore set out to investigate whether the CA1 projection in rats is equally selective in rat MEC and LEC and whether cortical and MS projections show preferential distributions to either one of the sublayers. Injecting the anterograde viral tracer, Tet-off lentivirus, into CA1 (n = 2), we confirmed and extended the previous observations in mice that axons originating in dorsal CA1 preferentially target LVb not only in MEC but also in LEC (Figure 2). We also confirmed a previous report that CA1 sends a weak projection to superficial layers of both entorhinal subdivisions (Cenquizca and Swanson, 2007; Kloosterman et al., 2003b). Injections into MS (n = 4) resulted in a densely labeled plexus in LII (Alonso and Köhler, 1984; Fuchs et al., 2016) as well as in LVa, whereas innervation of LVb was weak (Figure S2). In contrast, projections that arise from the ventral medial prefrontal cortex distribute in

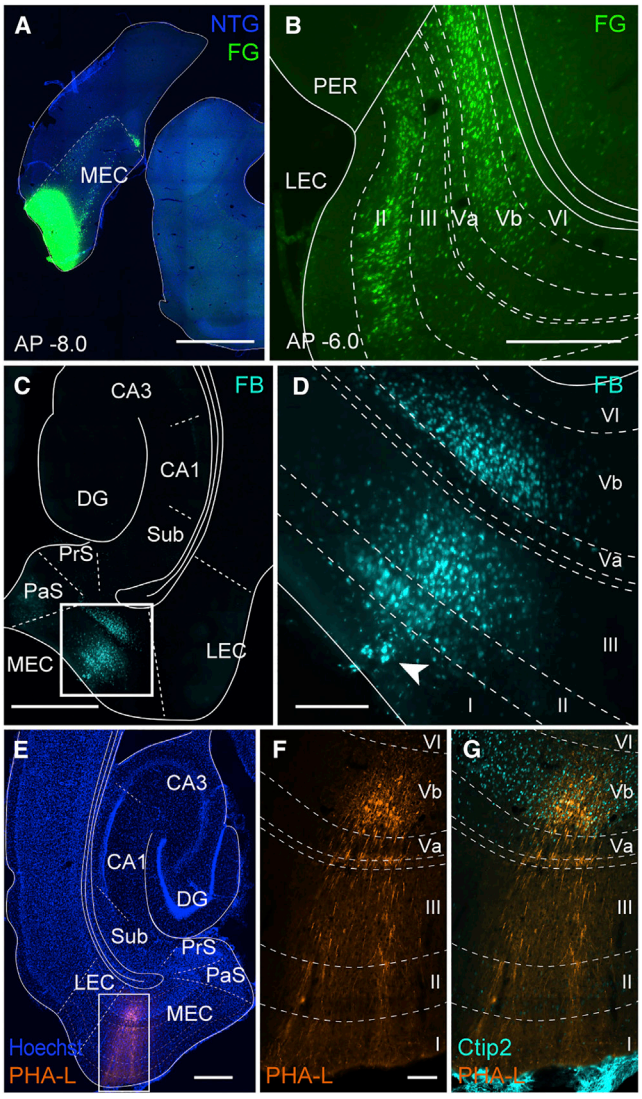

Figure 3. Local Projections of LVb Neurons

(A and B) Coronal sections showing that injection of the retrograde tracer FG in EC at AP = −8.0 (A) results in massive labeling of neurons in LVb and layers II and III in LEC at AP = −6.0 (B).

(C and D) Horizontal sections, taken at low (C) and high magnification (D), showing the selective distribution of retrogradely labeled neurons in LVb of MEC, following a Fast Blue (FB) injection into the superficial MEC (arrowhead in D points to the tip of the capillary used for injection).

(E) PHA-L injection into LVb of MEC resulted in anterogradely labeled axons in LII and LIII (horizontal section).

(F and G) High-magnification images of the boxed area in (E), illustrating the local, densely labeled projection in LII and LIII, without (F) and with the distribution of Ctip2 positive neurons (G).

The scale bars represent 2,000 μm for (A), 1,000 μm for (C), 500 μm for (B) and (E), and 100 μm for (D) and (F); scale bar in (F) also applies to (G).

LVb of both LEC and MEC, with a higher innervation density in LEC (n = 3; Figure S3). Projections from the retrosplenial cortex distribute selectively to MEC but, like the medial prefrontal projections, preferentially terminate in LVb (n = 4; Figure S4).

LVb Neurons Originate Intrinsic Projections Targeting Projection Neurons in LVa

For the mouse MEC, Sürmeli et al., (2015) hypothesized that LVb neurons might be the main origin of the well-known local projections within the entorhinal cortex and thus would innervate neurons in LVb. However, no experimental evidence for this was provided. To assess whether this suggestion is actually correct, we traced the origin of local projections in the entorhinal cortex. After large retrograde tracer injections into the superficial layers of EC at the border between LEC and MEC (n = 3), numerous labeled neurons were observed more anteriorly in LVb of LEC (Figures 3A and 3B). This supports that neurons in LVb are the main source of the long-range deep originating EC intrinsic connections reported previously (Dolorfo and Amaral, 1998). Small retrograde injections in the superficial layers (layers I–III) of MEC resulted in labeled LVb neurons, directly deep to the injection (Figures 3C and 3D), in line with a previously described column-like short-range projection arising from LV (van Haeften et al., 2003). To further examine the target layer of these local projections of LVb, we injected the anterograde tracer (PHA-L) into LVb of EC (Figures 3E–3G; n = 2). Such injections resulted in labeled axons that traversed LVa, the lamina dissecans, and the superficial layers, eventually reaching layer I. These results indicate that LVb neurons may innervate neurons in LVa, LIII, and LII.

To substantiate that LVb neurons indeed innervate neurons in LVa that project to telencephalic structures and neurons in LII and LIII projecting to the hippocampus, we conducted transsynaptic tracing experiments with rabies virus (RV). We used a glycoprotein-deleted RV vector (ΔG-RV), which, due to the lack of the gene encoding the glycoprotein, will only label the two sets of direct projecting neurons in LII, LIII, and LVa. In contrast, a CVS strain of RV (CVS-RV) can propagate transsynaptically and thus will additionally label neurons that make synaptic contacts with the 1st order infected projection neurons identified using ΔG-RV. We predicted that neurons in LVb are among this transsynaptically labeled population. We first assessed whether LVb neurons project to principal neurons in LVa (Figure 4) by injecting either one of the two rabies strains into NAc or RSC (Figures 4A and 4E). In animals with a ΔG-RV injection into NAc (n = 7), we observed many retrogradely labeled neurons in LVa but only few labeled neurons in other layers, including LVb (Figure 4B). A comparable pattern of labeling was observed following injections with CVS-RV injection with a short survival time (36 hr; data not shown). In contrast, sixty hours after a CVS-RV injection into NAc (n = 4), many labeled neurons were observed not only in LVa but also in LVb of both LEC and MEC (Figure 4C; Table S1). These labeled neurons in LVb were Ctip2 positive (Figure S5). The number of labeled LVb neurons in case of the CVS-RV experiments was significantly higher than in case of the ΔG-RV-injected samples ($p < 0.01$; Mann-Whitney U test; Figure 4D). This indicates that most of LVb neurons were transsynaptically labeled. Because LVb neurons do not project to NAc directly, as concluded based on the above described "classic" tracing experiments, these results strongly indicate that LVb neurons make mono-synaptic contacts with the NAc-projecting neurons in LVa. Injections of RV into RSC (n = 4 for ΔG-RV injection; n = 4 for CVS-RV

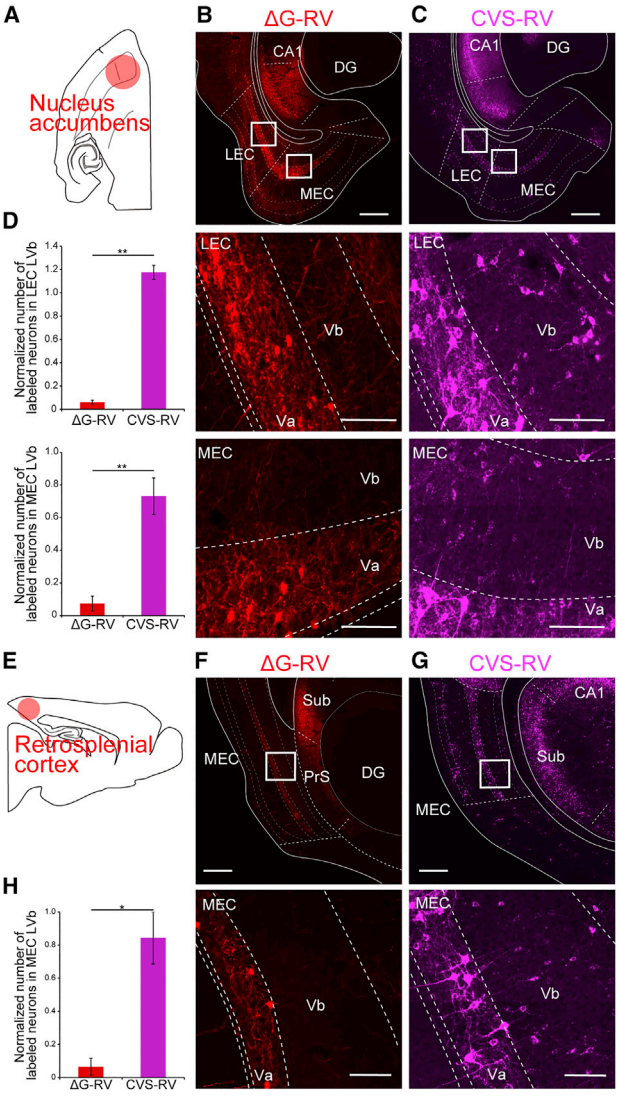

Figure 4. LVb Neurons Originate Intrinsic Projections to LVa Neurons

(A–C) Differential distribution of retrogradely labeled EC neurons in horizontal sections, after viral injection into the nucleus accumbens (NAc) (A) of either ΔG-RV (B) or CVS-RV (C). Note the higher number of labeled LVb neurons in (C) than in (B). The scale bars represent 500 μm for the low-magnification images (B and C, upper row) and 100 μm for the high-magnification images (B and C, lower rows). The position of the high-magnification images is indicated with the white boxes in the low-magnification images (upper row).

(D) Normalized number of labeled LVb neurons to labeled LVa neurons in both LEC (upper panel) and MEC (lower panel) after injection of ΔG-RV (n = 7) or CVS-RV (n = 4) into NAc (mean ± SEs; **p < 0.01; Mann-Whitney U test).

(E–G) Differential distribution of retrogradely labeled MEC neurons in sagittal sections after viral injection into the retrosplenial cortex (RSC) (E) of either ΔG-RV (F) or CVS-RV (G). Note the higher number of labeled LVb neurons in (C) than in (B). The scale bars represent 500 μm for the low-magnification images (F and G, upper row) and 100 μm for the high-magnification images (F and G, lower row). The position of the high-magnification images is indicated with the white boxes in the low-magnification images (upper row).

(H) Normalized number of labeled LVb neurons to labeled LVa neurons in MEC after injection of ΔG-RV (n = 4) and CVS-RV (n = 4) into RSC (mean ± SEM; *p < 0.05; Mann-Whitney U test).

injection) resulted in labeled neurons distributed predominantly in MEC, in line with the previous experiments and the literature (Burwell and Amaral, 1998). Similar to NAc injection samples, many labeled neurons were observed in MEC LVa in both ΔG-RV- and CVS-RV-injected samples (Figures 4F and 4G; Table S2). In contrast, the number of labeled LVb neurons increased significantly in case of CVS-RV injections compared with ΔG-RV cases ($p < 0.05$; Mann-Whitney U test; Figure 4H). These results thus indicate that MEC neurons in LVb are synaptically connected with the RSC-projecting MEC LVa neurons.

LVb Neurons Originate Intrinsic Projections Targeting Hippocampal-Projecting Neurons in LII and LIII

We next assessed whether LVb neurons target principal neurons in the superficial LII and LIII that project to the hippocampus. We injected the same pair of RV into the dorsal hippocampus involving both dentate gyrus (DG) and CA1 (Figure 5A). Injections of ΔG-RV into the hippocampus (n = 6) resulted in retrograde labeling in layer II and III of both LEC and MEC (Figure 5B). A very low number of labeled neurons were also present in layers Va, Vb, and VI, in line with previous reports about sparse hippocampal projections from layer V and VI neurons (Deller et al., 1996; Gloveli et al., 2001; Köhler, 1985b; Table S3). In contrast, in cases with CVS-RV injection (n = 4), in addition to labeling in the superficial layers, many labeled neurons were observed in LVb of both LEC and MEC (Figure 5C). The number of LVb-labeled cells, normalized over the total number of LII and LIII-labeled cells in each experimental animal, was significantly higher in CVS-RV-injected samples than in the ΔG-RV-injected samples in both LEC ($p < 0.01$; Mann-Whitney U test) and MEC ($p < 0.01$; Mann-Whitney U test; Figure 5D).

Similar to what we observed following ΔG-RV injections, we observed labeled neurons in LVa of both LEC and MEC following CVS-RV injections (Figure 5C; Table S3). The labeling of LVa neurons can thus reflect either direct projections or can be the result of transsynaptic labeling through their local projections to the superficial layers (Canto and Witter, 2012a, 2012b), although we cannot exclude that some LVa neurons were labeled transsynaptically through other possible extrahippocampal targets, such as the thalamic nucleus of reuniens (Herkenham, 1978) or the septum (Alonso and Köhler, 1984). Because we have shown that LVb neurons do not project to brain targets outside the entorhinal cortex, our data support the conclusion that the LVb neurons were transsynaptically labeled by way of the hippocampal-projecting neurons located in superficial layers II and III.

DISCUSSION

It is well-established that neurons in entorhinal LV are the recipients of hippocampal output originating in CA1 and subiculum (Cenquizca and Swanson, 2007; Kloosterman et al., 2003b; Köhler, 1985a). Recently, an interesting detail was added in mouse MEC, that in particular, entorhinal LVb neurons are the main recipients of the hippocampal projections but that they essentially lack projections to telencephalic structures (Sürmeli et al., 2015). In our study, we confirmed in the rat that LVb neurons do not project to telencephalic regions, in accordance with previously

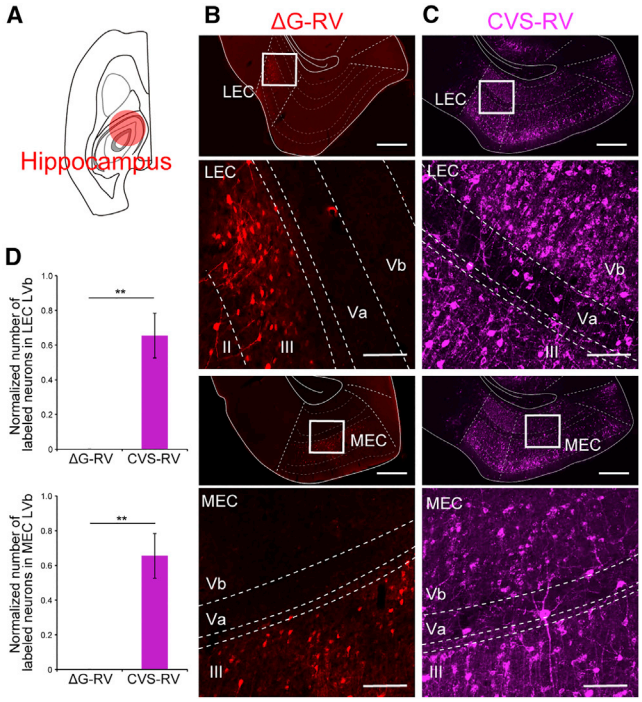

Figure 5. LVb Originate Intrinsic Projections to Hippocampus-Projecting LII/LIII Neurons

(A–C) Differential distribution of retrogradely labeled EC neurons in horizontal sections after viral injection into the hippocampus (A) of either ΔG-RV (B) or CVS-RV (C). Note the dramatic increase in number of labeled LVb neurons in (C) over that seen in (B). The scale bars represent 500 μm for the low-magnification images and 100 μm for the high-magnification images. The position of the high-magnification images is indicated with white boxes in the low-magnification images.

(D) Normalized number of labeled LVb neurons to labeled LII and LIII neurons for ΔG-RV-infected samples (n = 6) and CVS-RV-infected samples (n = 4) in both LEC (upper panel) and MEC (lower panel; mean ± SEM; **$p < 0.01$; Mann-Whitney U test).

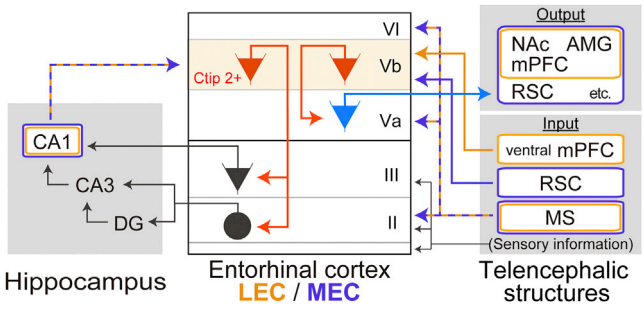

Figure 6. Summary of the Connectivity of LVa and LVb in LEC and MEC

LVa and LVb neurons are connectionally different in both MEC and LEC. EC LVa neurons project to telencephalic structures, whereas LVb neurons project locally to telencephalic-projecting LVa neurons and also to hippocampus-projecting LII and LIII neurons. Also indicated are differences in the inputs to LVa and LVb of MEC (purple) and LEC (yellow) from CA1, mPFC, RSC, and MS.

published data in the mouse, but we could not replicate that MEC LVb neurons project to the anterior thalamus (Sürmeli et al., 2015). Our major finding is that LVb neurons in both MEC and LEC mediate two circuits in the hippocampus-memory system: a hippocampal output circuit to telencephalic areas by projecting to LVa and a feedback loop by projecting back to the EC-hippocampal loop via neurons in LII and LIII (Figure 6). Our findings thus position LVb neurons as key elements of these two networks of the entorhinal cortex.

Our experimental data, based on transsynaptic tracing, prove the postulate that LVb neurons originate intrinsic connections within MEC (Sürmeli et al., 2015) correct by showing that indeed LVb cells send axons toward layers Va, III, and II. We further show that this holds true not only in MEC but also in LEC. We thus conclude that the hippocampal-cortical output circuit and the hippocampal re-entry circuit are not simple disynaptic pathways but more complicated trisynaptic pathways, including a third synapse involving LVb neurons. We argue that the transsynaptic labeling is due to the transsynaptic spread of RV via EC neurons in layers II, III and Va. The labeling of LVb neurons might be the result of indirect multisynaptic labeling through interneurons that target principal neurons in LVa, LII, and LIII. We deem this unlikely in view of the limited survival time (Iwata et al., 2011; Kelly and Strick, 2003; Miyachi et al., 2005, 2006) and, in case of LII and LIII, the fact that the majority of postsynaptic targets of local projections from LV to superficial layers are spiny principal neurons (van Haeften et al., 2003).

Previous studies have shown LV projections to superficial LII and LIII without differentiating between a potential preferred origin in LVb over LVa (van Haeften et al., 2003; Czajkowski et al., 2013; Dolorfo and Amaral, 1998). Both anatomical and electrophysiological studies indicated that these projections mainly originate from excitatory neurons (Gloveli et al., 1997; van Haeften et al., 2003) and that the net effect of activation of LV neurons is the generation of excitatory responses in layers II and III principal neurons (Iijima et al., 1996; Kloosterman et al., 2003a). It is thus likely that the labeled LVb neurons, which we observed in this study, are excitatory neurons. Thus, the information that is processed through the hippocampus will be sent back to the hippocampus through this excitatory entorhinal-hippocampal loop. Although the function of this re-entrant activity (reverberation) has not been examined directly, it is thought that this is one of the mechanisms underlying temporal storage of information in neuronal networks. However, it must be noted that, irrespective of the above-mentioned net excitatory effects, 44% of the excitatory deep-to-superficial projections make synapses on non-spiny dendritic shafts, indicative for interneurons as postsynaptic partners (van Haeften et al., 2003). It remains to be established how these excitatory and feedforward inhibitory inputs cooperatively influence the re-entry circuit and whether the deep-to-superficial inputs differ depending on whether they target DG/CA3/2-projecting LII neurons or CA1/sub-projecting LIII neurons (Iijima et al.,1996).

Our findings indicate that the hippocampal-cortical output circuit, like the hippocampal re-entry circuit, is not simple disynaptic pathways but more complicated trisynaptic pathways, mediated by neurons in LVb. What we do not know yet is whether the same neuron in LVb is involved in both pathways or acts as a

selective component of one of the two. Irrespective of this, the connectional distinction of the two LV sublayers in both LEC and MEC allows for a selective modification of the output circuit mediated by LVb and LVa without affecting the hippocampal re-entry circuit mediated by LVb, LII, and LIII or vice versa. In this perspective, it is of critical relevance to assess at which layer main modulatory systems target the entorhinal cortex. One of the most studied inputs in this respect originates in MS, known to be critically involved in synchronization between hippocampal and parahippocampal structures in the theta frequency band (Lopes da Silva et al., 1990). Although much focus has been on the role of this complex with respect to theta generation in LII of MEC (Deshmukh et al., 2010; Jeewajee et al., 2008; Tahvildari and Alonso, 2005), we show that projections also target deeper layers of both LEC and MEC, showing a striking preference for LVa, corroborating previously published findings (Gonzalez-Sulser et al., 2014). Interestingly, projections from the claustrum also preferentially terminate more heavily in LVa and VI than in LVb (Eid et al., 1996; Kitanishi and Matsuo, 2017). The preferred input to LVa may control the gating of the information flow from the hippocampus to the neocortex. This notion is supported by reports that the projection from MEC LVa to medial prefrontal cortex is crucial for remote memory of contextual fear conditioning (Kitamura et al., 2017) and that this process depends on the claustrum (Kitanishi and Matsuo, 2017). The latter authors reported that inactivating the input from the claustrum to MEC LVa impaired the long-term memory retrieval of a contextual fear memory. In contrast, cortical inputs arising from the medial prefrontal cortex and the retrosplenial cortex show a clear preference for LVb of LEC and/or MEC. These inputs thus likely influence both hippocampal-EC LVb-mediated projections in a similar way, because preliminary data indicate that, in case of MEC, inputs from RSC and subiculum converge on neurons in LVb (Simonsen et al., 2012, FENS, abstract).

In this study, we conclude that LVb neurons of LEC and MEC constitute local circuit elements, involved in both the hippocampal re-entry circuit via LII and LIII and the hippocampal-output circuit via LVa. The fact that both LEC and MEC share this unique feature of having a sublayer of LV neurons dedicated to short- and long-range intrinsic connections to both of the main entorhinal projection systems is exceptional for cortex. In the neocortex, neurons in deep layer V (Vb) give rise to descending projections to brainstem structures and striatum, whereas projections from more superficial neurons (Va) seem to selectively originate inter-telencephalic and local projections, with a subclass projecting also to the striatum (Gerfen et al., 2016; Kim et al., 2015; Shipp, 2007). Whether the specific connectivity of LVb in EC is related to the overall unique organization of EC, lacking strong descending projections, and originates not only the canonical cortical projection systems from layers V, III, and II but also the massive hippocampal projections from LII and LIII (Witter et al., 2017) remains to be elucidated.

EXPERIMENTAL PROCEDURES

Surgical Procedures

Young adult male Wistar rats weighing 200–250 g were used in this study. All experiments were approved by the Center for Laboratory Animal Research, Tohoku University Guidelines for Animal Care and Use. For the viral experiments, we set clinical signs of rabies (slow and circular movements, paralysis, and cachexia) as humane endpoints. However, because none of the rats showed any clinical signs of rabies, they were all sacrificed with an overdose of sodium pentobarbital after a certain survival time in accordance with the experimental schedule. All experiments requiring injections of RV and RV vectors were carried out in a special laboratory (biosafety level 2) designed for *in vivo* infectious experiments.

Rats were deeply anaesthetized with ketamine (60 mg/kg, intraperitoneally [i.p.]) and xylazine (4.8 mg/kg, i.p.) and were mounted in a stereotaxic frame. The skull was exposed, and a small burr hole was drilled above the injection site. The injection was made by means of a glass micropipette (tip diameter = 20–40 μm) connected to 1 μL Hamilton microsyringe. Coordinates of following injection sites were based on the rat brain atlas (Paxinos and Watson, 2007) and calculated from bregma.

For retrograde tracing experiments, rats received injection of 100 nL of either 1.25% Fluoro-Gold (Fluorochrome) or 1 mg/mL Alexa-Fluor-555-conjugated cholera toxin subunit B (CTB555; Thermo Fisher Scientific) into either the BLA (AP = −2.5; ML = 5.0; DV = −6.7), NAc (AP = +2.0; ML = 1.6; DV = −6.1), PrL (AP = +3.0; ML = 0.6; DV = −3.3), RSC (AP = −7.7; ML = 0.75; DV = −1.45), anterior thalamus (AP = −1.6; ML = 1.2; DV = −5.4), laterodorsal thalamic nucleus (AP = −2.4; ML = 2.3; DV = −4.4), or EC (AP = −8.3; ML = 6.0; DV = −3.95) at the rate of 20 nL per minute. The pipette was left in place for another 15 min before it was withdrawn. For anterograde tracing experiments, 2.5% Phaseolus vulgaris-leucoagglutinin (PHA-L; Vector Laboratories) was injected into EC LVb (0.7 mm anterior from front edge of transverse sinus; ML = 5.2; DV = −3.5; angle of 20° in the coronal plane) iontophoretically with positive 5 μA current pulses (6 s on; 6 s off) for 15 min. For the animal that received dual tracer injections, 150 nL of 1% Fast Blue (EMS-Chemie) was injected into the superficial MEC (1.3 mm anterior from the transverse sinus; ML = 4.6; DV = −4.8 mm), whereas 2.5% PHA-L was iontophoretically injected into the RSC (1.0 mm anterior from the transverse sinus; ML = 2.1; DV = −1.2, −1.5, and −1.8 mm) with a positive pulsed direct current (current 7.5 μA; 6 s on; 6 s off) for 10 min.

For retrograde viral tracing, rats received injection of either 100–200 nL of G-deleted rabies viral vector (rHEP5.0-ΔG-mRFP; 6.0×10^8 focus forming units (FFU)/mL; Ohara et al., 2013) or propagation-competent rabies virus (challenge virus standard [CVS] strain; 2.6×10^7 FFU/mL, supplied by Dr. Kinjiro Morimoto, National Institute of Infectious Diseases, Japan) into either NAc, RSC, or hippocampus (AP = −3.2; ML = 2.0; DV = −2.6 and −2.2) at the rate of 20 nL per minute. Each virus was injected with 1% of pontamine sky blue in order to mark the injection sites. For anterograde viral tracing, rats received injections of 1,500 nL of Tet-Off lentiviruses (Hioki et al., 2009), a mixture of STB (2.6×10^{12} copy number of the RNA genome/mL) and TpGB (6.7×10^{11} copy number of the RNA genome/mL) into either CA1 (AP = −3.8; ML = 3.1; DV = −2.3), MS (AP = +0.4; ML = 1.6; DV = −6.4), or infralimbic cortex (IL) (AP = +3.0; ML = 0.6; DV = −3.3) at the rate of 150 nL/min. In each experiment, the micropipette was left in place for an additional 15 min after the injection, before it was slowly withdrawn from the brain. When all injections were completed, the wound was sutured and the animal was monitored for recovery from anesthesia and returned to its home cage. Throughout the survival times, all rats were kept inside a small safety cabinet.

Immunohistochemistry and Analysis

All rats that received injection of chemical tracers and rHEP5.0-ΔG-mRFP were sacrificed after 7 days of survival periods, whereas rats that received Tet-Off lentivirus injection were sacrificed 14 days after surgery. For the rats that received injection of the CVS strain, we strictly adjusted the survival time in order to control the spread of the virus. Previous virus-tracing studies using the CVS strain have reported that it takes two days for this virus to retrogradely infect and label the neurons that have direct inputs to the injection site (1st order neurons) and another one day to transport one synapse and transsynaptically label the presynaptic neurons (2nd order neurons; Iwata et al., 2011; Kelly and Strick, 2003; Miyachi et al., 2005, 2006). Because we observed transsynaptic labeling of 2nd order neurons in samples with 2.5 days of survival and not in samples with survival time of 1.5 or 2 days,

we used a survival time of the CVS-RV-injected rats of 2.5 days in this study. After the appropriate survival periods, the animals were deeply anaesthetized with sodium pentobarbital (100 mg/kg, i.p.) and transcardially perfused and fixed with 10% sucrose in 0.1 M phosphate buffer (PB) (pH 7.4) followed by 4% freshly prepared paraformaldehyde in 0.1M PB. The brains were removed from the skulls, postfixed in the same fresh fixative for 4 hr at 4°C, and then cryoprotected for at least 48 hr at 4°C in PB containing 30% sucrose. The brains were coronally, horizontally, or sagittally sectioned at 40 μm on a freezing microtome.

The Ctip2- and PCP4-positive neurons, anterograde labeling, and the RV-infected neurons were visualized by immunostaining as described below. All brain sections were soaked in PBS containing 5% goat serum and 0.1% Triton X-100 (blocking solution) for an hour at room temperature. Sections were then incubated overnight at 4°C with primary antibodies diluted in the same blocking solution. Sections were subsequently washed three times with PBS containing 0.1% Triton X-100 (PBT) and incubated with secondary antibodies diluted in PBT for 4 hr at room temperature. The sections were counterstained with NeuroTrace 500/525 green fluorescent Nissl stain (1:250; Thermo Fisher Scientific) or Hoechst 33258 (1:1,000; Dojindo), washed three times with PBS, mounted onto gelatin-coated glass slides, air-dried, soaked in xylene, and coverslipped with mounting medium (Entellan new; Merck Millipore). The following antibodies were used in this study: anti-Ctip2 rat immunoglobulin G (IgG) (1:250; Abcam; ab18465); anti-PCP4 rabbit IgG (1:250; Sigma; HPA005792); anti-GFP rabbit IgG (1:400; Life Technologies; A11122); anti-GFP mouse IgG (1:400; Invitrogen; A-11120); anti-PHA-L rabbit IgG (1:800; Vector Laboratories); anti-DsRed rabbit IgG (1:400; Clontech Laboratories; 632496); and monospecific rabbit anti-N antiserum (1:25,000; supplied by Dr. Satoshi Inoue, National Institute of Infectious Diseases, Japan; Inoue et al., 2003) as primary antibodies and Alexa-Fluor-647-conjugated anti-rat; goat IgG (1:400; Jackson ImmunoResearch); Cy5-conjugated anti-rabbit goat IgG (1:400; Jackson ImmunoResearch); Alexa-488-conjugated anti-mouse goat IgG (1:400; Jackson ImmunoResearch); and Cy3-conjugated anti-rabbit goat IgG (1:400; Jackson ImmunoResearch) as secondary antibodies. Sections were examined using an Axiovert 200 M microscope (Carl Zeiss) and imaged either with a laser scanning confocal unit (LSM 5 Exciter; Carl Zeiss) or with a digital camera (AxioCam MRm). Axio Scan. Z1 (Carl Zeiss) and ZEN 2 software (Carl Zeiss) were also used to image the labeled neurons.

The numbers of RV-infected neurons in LII, LIII, and LV of LEC and MEC were counted in every section from one series, which were obtained with 240 μm distance. In samples with NAc and RSC injection, the number of labeled LVb neurons was normalized on the basis of the total number of labeled LVa neurons in each sample. In samples with hippocampus injection, the number of labeled LVb neurons was normalized to that of labeled LII and LIII neurons. All numerical data are expressed as mean values ± the SEM. The statistical significance between direct and transsynaptic inputs was evaluated by using Mann-Whitney U test.

SUPPLEMENTAL INFORMATION

Supplemental Information includes five figures and three tables and can be found with this article online at https://doi.org/10.1016/j.celrep.2018.06.014.

ACKNOWLEDGMENTS

We thank Dr. Satoshi Inoue (National Institute of Infectious Diseases, Japan) for kindly supplying the monospecific rabbit anti-N antiserum and Dr. Kinjiro Morimoto (National Institute of Infectious Diseases, Japan) for kindly supplying the rabies virus (challenge virus standard strain). This study was supported by Grants-in-Aid for Scientific Research on Innovative Areas (16H01495) and by Grant-in-Aid for Scientific Research (KAKENHI) 15K18358 from the Ministry of Education, Culture, Sports, Science and Technology (MEXT) of Japan. It was also supported by the Research Council of Norway: the Centre of Excellence scheme-Centre for Neural Computation (grant no. 223262), the National Infrastructure scheme–NORBRAIN (grant no. 197467), research grant no. 227769, and The Egil and Pauline Braathen and Fred Kavli Centre for Cortical Microcircuits. This study was partially supported by MEXT/JSPS (16H04663, 17K19451, 15H01430, and 16H01426) and by Brain/MINDS from AMED (JP18dm0207064 to H.H.).

AUTHOR CONTRIBUTIONS

S.O. and M.P.W. conceived the study design. M.O., S.O., Ø.W.S., and R.Y. collected and analyzed the experimental data. All quantifications were carried out by M.O. All authors contributed to the discussions that resulted in the current paper, which was written by S.O., M.O., and M.P.W. All authors approved the final version of the manuscript.

DECLARATION OF INTERESTS

The authors declare no competing interests.

Received: December 11, 2017
Revised: May 4, 2018
Accepted: June 1, 2018
Published: July 3, 2018

REFERENCES

Agster, K.L., and Burwell, R.D. (2009). Cortical efferents of the perirhinal, postrhinal, and entorhinal cortices of the rat. Hippocampus *19*, 1159–1186.

Alonso, A., and Köhler, C. (1984). A study of the reciprocal connections between the septum and the entorhinal area using anterograde and retrograde axonal transport methods in the rat brain. J. Comp. Neurol. *225*, 327–343.

Burwell, R.D., and Amaral, D.G. (1998). Cortical afferents of the perirhinal, postrhinal, and entorhinal cortices of the rat. J. Comp. Neurol. *398*, 179–205.

Buzsáki, G. (1996). The hippocampo-neocortical dialogue. Cereb. Cortex *6*, 81–92.

Canto, C.B., and Witter, M.P. (2012a). Cellular properties of principal neurons in the rat entorhinal cortex. I. The lateral entorhinal cortex. Hippocampus *22*, 1256–1276.

Canto, C.B., and Witter, M.P. (2012b). Cellular properties of principal neurons in the rat entorhinal cortex. II. The medial entorhinal cortex. Hippocampus *22*, 1277–1299.

Canto, C.B., Wouterlood, F.G., and Witter, M.P. (2008). What does the anatomical organization of the entorhinal cortex tell us? Neural Plast. *2008*, 381243.

Cappaert, N.L.M., Van Strien, N.M., and Witter, M.P. (2015). Hippocampal formation. In The Rat Nervous System, Fourth Edition, G. Paxinos, ed. (Elsevier), pp. 511–573.

Cenquizca, L.A., and Swanson, L.W. (2007). Spatial organization of direct hippocampal field CA1 axonal projections to the rest of the cerebral cortex. Brain Res. Brain Res. Rev. *56*, 1–26.

Czajkowski, R., Sugar, J., Zhang, S.-J., Couey, J.J., Ye, J., and Witter, M.P. (2013). Superficially projecting principal neurons in layer V of medial entorhinal cortex in the rat receive excitatory retrosplenial input. J. Neurosci. *33*, 15779–15792.

Deller, T., Martinez, A., Nitsch, R., and Frotscher, M. (1996). A novel entorhinal projection to the rat dentate gyrus: direct innervation of proximal dendrites and cell bodies of granule cells and GABAergic neurons. J. Neurosci. *16*, 3322–3333.

Deshmukh, S.S., Yoganarasimha, D., Voicu, H., and Knierim, J.J. (2010). Theta modulation in the medial and the lateral entorhinal cortices. J. Neurophysiol. *104*, 994–1006.

Dolorfo, C.L., and Amaral, D.G. (1998). Entorhinal cortex of the rat: organization of intrinsic connections. J. Comp. Neurol. *398*, 49–82.

Edelman, G.M. (1989). The Remembered Present: A Biological Theory of Consciousness (Basic Books), p. 272.

Eichenbaum, H., Sauvage, M., Fortin, N., Komorowski, R., and Lipton, P. (2012). Towards a functional organization of episodic memory in the medial temporal lobe. Neurosci. Biobehav. Rev. *36*, 1597–1608.

Eid, T., Jorritsma-Byham, B., Schwarcz, R., and Witter, M.P. (1996). Afferents to the seizure-sensitive neurons in layer III of the medial entorhinal area: a tracing study in the rat. Exp. Brain Res. *109*, 209–218.

Fuchs, E.C., Neitz, A., Pinna, R., Melzer, S., Caputi, A., and Monyer, H. (2016). Local and distant input controlling excitation in layer II of the medial entorhinal cortex. Neuron *89*, 194–208.

Gerfen, C.R., Economo, M.N., and Chandrashekar, J. (2016). Long distance projections of cortical pyramidal neurons. J. Neurosci. Res. Published online November 12, 2016. https://doi.org/10.1002/jnr.23978.

Gloveli, T., Schmitz, D., Empson, R.M., and Heinemann, U. (1997). Frequency-Dependent Information Flow From the Entorhinal Cortex to the Hippocampus. J. Neurophysiol. *78*, 3444–3449.

Gloveli, T., Dugladze, T., Schmitz, D., and Heinemann, U. (2001). Properties of entorhinal cortex deep layer neurons projecting to the rat dentate gyrus. Eur. J. Neurosci. *13*, 413–420.

Gonzalez-Sulser, A., Parthier, D., Candela, A., McClure, C., Pastoll, H., Garden, D., Sürmeli, G., and Nolan, M.F. (2014). GABAergic projections from the medial septum selectively inhibit interneurons in the medial entorhinal cortex. J. Neurosci. *34*, 16739–16743.

Hamam, B.N., Kennedy, T.E., Alonso, A., and Amaral, D.G. (2000). Morphological and electrophysiological characteristics of layer V neurons of the rat medial entorhinal cortex. J. Comp. Neurol. *418*, 457–472.

Hamam, B.N., Amaral, D.G., and Alonso, A.A. (2002). Morphological and electrophysiological characteristics of layer V neurons of the rat lateral entorhinal cortex. J. Comp. Neurol. *451*, 45–61.

Hasselmo, M.E. (2013). Neuronal rebound spiking, resonance frequency and theta cycle skipping may contribute to grid cell firing in medial entorhinal cortex. Philos. Trans. R. Soc. Lond. B Biol. Sci. *369*, 20120523.

Herkenham, M. (1978). The connections of the nucleus reuniens thalami: evidence for a direct thalamo-hippocampal pathway in the rat. J. Comp. Neurol. *177*, 589–610.

Hioki, H., Kuramoto, E., Konno, M., Kameda, H., Takahashi, Y., Nakano, T., Nakamura, K.C., and Kaneko, T. (2009). High-level transgene expression in neurons by lentivirus with Tet-Off system. Neurosci. Res. *63*, 149–154.

Iijima, T., Witter, M.P., Ichikawa, M., Tominaga, T., Kajiwara, R., and Matsumoto, G. (1996). Entorhinal-hippocampal interactions revealed by real-time imaging. Science *272*, 1176–1179.

Inoue, S., Sato, Y., Hasegawa, H., Noguchi, A., Yamada, A., Kurata, T., and Iwasaki, T. (2003). Cross-reactive antigenicity of nucleoproteins of lyssaviruses recognized by a monospecific antirabies virus nucleoprotein antiserum on paraffin sections of formalin-fixed tissues. Pathol. Int. *53*, 525–533.

Insausti, R., Herrero, M.T., and Witter, M.P. (1997). Entorhinal cortex of the rat: cytoarchitectonic subdivisions and the origin and distribution of cortical efferents. Hippocampus *7*, 146–183.

Iwata, K., Miyachi, S., Imanishi, M., Tsuboi, Y., Kitagawa, J., Teramoto, K., Hitomi, S., Shinoda, M., Kondo, M., and Takada, M. (2011). Ascending multisynaptic pathways from the trigeminal ganglion to the anterior cingulate cortex. Exp. Neurol. *227*, 69–78.

Jeewajee, A., Barry, C., O'Keefe, J., and Burgess, N. (2008). Grid cells and theta as oscillatory interference: electrophysiological data from freely moving rats. Hippocampus *18*, 1175–1185.

Jones, B.F., and Witter, M.P. (2007). Cingulate cortex projections to the parahippocampal region and hippocampal formation in the rat. Hippocampus *17*, 957–976.

Kelly, R.M., and Strick, P.L. (2003). Cerebellar loops with motor cortex and prefrontal cortex of a nonhuman primate. J. Neurosci. *23*, 8432–8444.

Kerr, K.M., Agster, K.L., Furtak, S.C., and Burwell, R.D. (2007). Functional neuroanatomy of the parahippocampal region: the lateral and medial entorhinal areas. Hippocampus *17*, 697–708.

Kim, E.J., Juavinett, A.L., Kyubwa, E.M., Jacobs, M.W., and Callaway, E.M. (2015). Three types of cortical layer 5 neurons that differ in brain-wide connectivity and function. Neuron *88*, 1253–1267.

Kitamura, T., Ogawa, S.K., Roy, D.S., Okuyama, T., Morrissey, M.D., Smith, L.M., Redondo, R.L., and Tonegawa, S. (2017). Engrams and circuits crucial for systems consolidation of a memory. Science *356*, 73–78.

Kitanishi, T., and Matsuo, N. (2017). Organization of the claustrum-to-entorhinal cortical connection in mice. J. Neurosci. *37*, 269–280.

Kloosterman, F., Van Haeften, T., Witter, M.P., and Lopes Da Silva, F.H. (2003a). Electrophysiological characterization of interlaminar entorhinal connections: an essential link for re-entrance in the hippocampal-entorhinal system. Eur. J. Neurosci. *18*, 3037–3052.

Kloosterman, F., Witter, M.P., and Van Haeften, T. (2003b). Topographical and laminar organization of subicular projections to the parahippocampal region of the rat. J. Comp. Neurol. *455*, 156–171.

Knierim, J.J. (2015). The hippocampus. Curr. Biol. *25*, R1116–R1121.

Köhler, C. (1985a). Intrinsic projections of the retrohippocampal region in the rat brain. I. The subicular complex. J. Comp. Neurol. *236*, 504–522.

Köhler, C. (1985b). A projection from the deep layers of the entorhinal area to the hippocampal formation in the rat brain. Neurosci. Lett. *56*, 13–19.

Köhler, C. (1986). Intrinsic connections of the retrohippocampal region in the rat brain. II. The medial entorhinal area. J. Comp. Neurol. *246*, 149–169.

Köhler, C. (1988). Intrinsic connections of the retrohippocampal region in the rat brain: III. The lateral entorhinal area. J. Comp. Neurol. *271*, 208–228.

Lopes da Silva, F.H., Witter, M.P., Boeijinga, P.H., and Lohman, A.H. (1990). Anatomic organization and physiology of the limbic cortex. Physiol. Rev. *70*, 453–511.

Miyachi, S., Lu, X., Inoue, S., Iwasaki, T., Koike, S., Nambu, A., and Takada, M. (2005). Organization of multisynaptic inputs from prefrontal cortex to primary motor cortex as revealed by retrograde transneuronal transport of rabies virus. J. Neurosci. *25*, 2547–2556.

Miyachi, S., Lu, X., Imanishi, M., Sawada, K., Nambu, A., and Takada, M. (2006). Somatotopically arranged inputs from putamen and subthalamic nucleus to primary motor cortex. Neurosci. Res. *56*, 300–308.

Ohara, S., Sato, S., Oyama, K., Tsutsui, K., and Iijima, T. (2013). Rabies virus vector transgene expression level and cytotoxicity improvement induced by deletion of glycoprotein gene. PLoS ONE *8*, e80245.

Paxinos, G., and Watson, C. (2007). The Rat Brain in Stereotaxic Coordinates, Sixth Edition (Elsevier).

Ramsden, H.L., Sürmeli, G., McDonagh, S.G., and Nolan, M.F. (2015). Laminar and dorsoventral molecular organization of the medial entorhinal cortex revealed by large-scale anatomical analysis of gene expression. PLoS Comput. Biol. *11*, e1004032.

Shipp, S. (2007). Structure and function of the cerebral cortex. Curr. Biol. *17*, R443–R449.

Sugar, J., Witter, M.P., van Strien, N.M., and Cappaert, N.L. (2011). The retrosplenial cortex: intrinsic connectivity and connections with the (para)hippocampal region in the rat. An interactive connectome. Front. Neuroinform. *5*, 7.

Sürmeli, G., Marcu, D.C., McClure, C., Garden, D.L.F., Pastoll, H., and Nolan, M.F. (2015). Molecularly defined circuitry reveals input-output segregation in deep layers of the medial entorhinal cortex. Neuron *88*, 1040–1053.

Tahvildari, B., and Alonso, A. (2005). Morphological and electrophysiological properties of lateral entorhinal cortex layers II and III principal neurons. J. Comp. Neurol. *491*, 123–140.

Tang, Q., Ebbesen, C.L., Sanguinetti-Scheck, J.I., Preston-Ferrer, P., Gundlfinger, A., Winterer, J., Beed, P., Ray, S., Naumann, R., Schmitz, D., et al. (2015). Anatomical organization and spatiotemporal firing patterns of layer 3 neurons in the rat medial entorhinal cortex. J. Neurosci. *35*, 12346–12354.

van Haeften, T., Baks-te-Bulte, L., Goede, P.H., Wouterlood, F.G., and Witter, M.P. (2003). Morphological and numerical analysis of synaptic interactions between neurons in deep and superficial layers of the entorhinal cortex of the rat. Hippocampus *13*, 943–952.

Vertes, R.P., Linley, S.B., Groenewegen, H.J., and Witter, M.P. (2015). Thalamus. In The Rat Nervous System, Fourth Edition, G. Paxinos, ed. (Elsevier), pp. 335–390.

Witter, M.P., Groenewegen, H.J., Lopes da Silva, F.H., and Lohman, A.H.M. (1989). Functional organization of the extrinsic and intrinsic circuitry of the parahippocampal region. Prog. Neurobiol. *33*, 161–253.

Witter, M.P., Doan, T.P., Jacobsen, B., Nilssen, E.S., and Ohara, S. (2017). Architecture of the entorhinal cortex A review of entorhinal anatomy in rodents with some comparative notes. Front. Syst. Neurosci. *11*, 46.

Cell Reports, Volume *24*

Supplemental Information

Intrinsic Projections of Layer Vb Neurons to Layers Va, III, and II in the Lateral and Medial Entorhinal Cortex of the Rat

Shinya Ohara, Mariko Onodera, Øyvind W. Simonsen, Rintaro Yoshino, Hiroyuki Hioki, Toshio Iijima, Ken-Ichiro Tsutsui, and Menno P. Witter

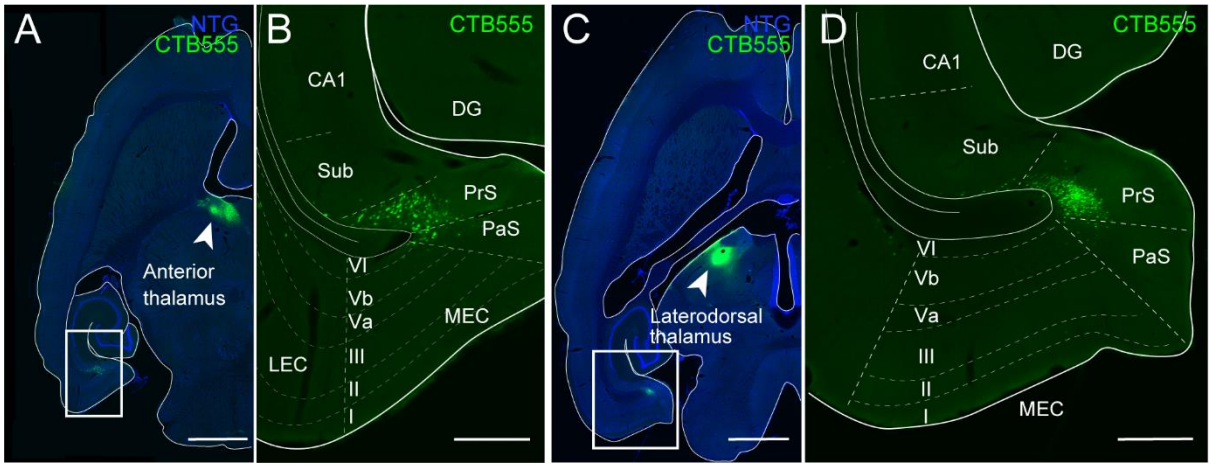

Figure S1. Absence of projections from EC to anterior and laterodorsal thalamus.

(A–B) Horizontal sections showing numerous retrogradely labeled neurons in deep layers of presubiculum (PrS) and parasubiculum (PaS) (B, boxed area in A) after CTB555 injection into anterior thalamus (white arrowhead in A). Note that no labeling is present in EC.

(C–D) Horizontal sections showing many retrogradely labeled neurons in deep layers of PrS (C, boxed area in D) after CTB555 injection into laterodorsal thalamus (white arrowhead in C). Note that no labeling is present in EC. Scale bars are 2000 μm for (A) and (C), and 500 μm for (B) and (C). CA1, subdivision of the hippocampus; DG, dentate gyrus; Sub, subiculum.

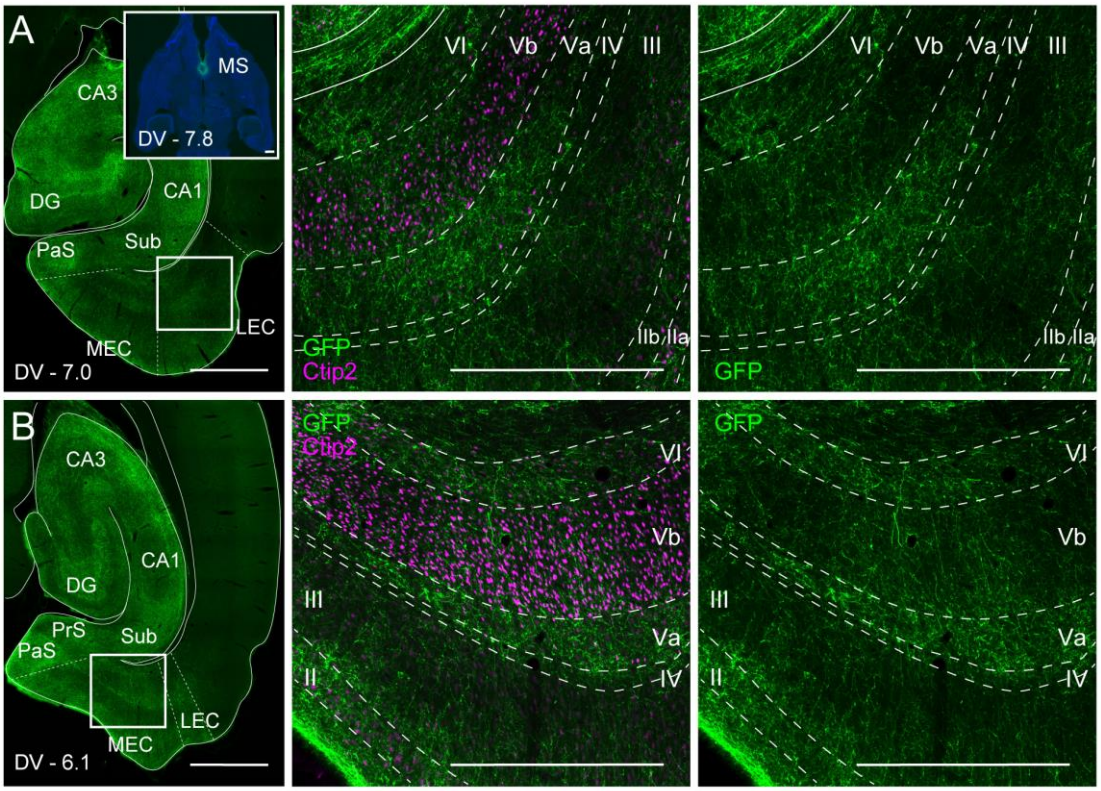

Figure S2. Inputs from the medial septum complex (MS) to EC preferentially terminate in LVa.

Distribution of GFP-labeled fibers (green) in LEC (A) and MEC (B) following a Tet-off lentiviral vector injection into MS. Left-hand panels show low magnification images of the hippocampal region in horizontal sections (scale bars are 1000 μm). Inset shows the injection site in a section counterstained with Hoechst (blue). The middle and right-hand panels represent the boxed areas in LEC and MEC with and without staining for the transcription factor Ctip2, marking neurons in LVb (magenta; scale bars are 500 μm).

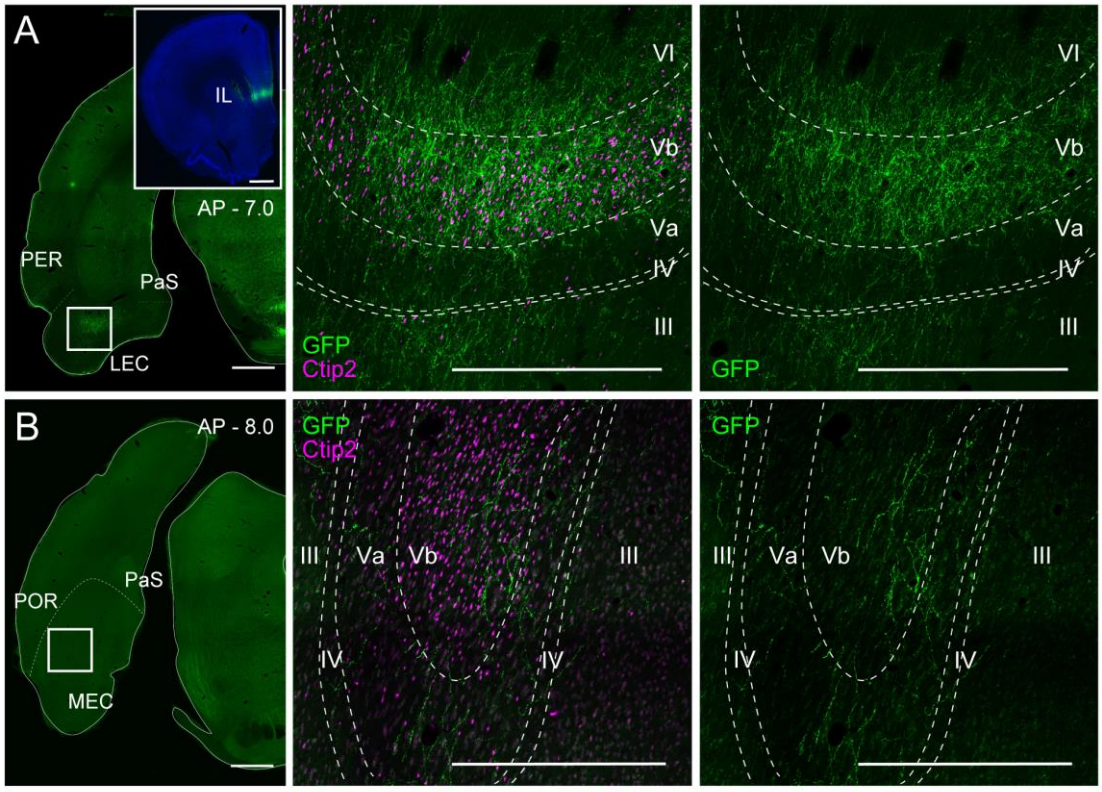

Figure S3. Projections from ventral medial prefrontal cortex (mPFC) to LV of LEC and MEC preferentially terminate in LVb.

Distribution of GFP-labeled fibers (green) in LEC (A) and MEC (B) following a Tet-off lentiviral vector injection into ventral mPFC. Left-hand panels show low magnification images of the hippocampal region in coronal sections (scale bars are 1000 μm). Inset shows the injection site in a section counterstained by Hoechst (blue). The middle and right-hand panels represent the boxed areas in LEC and MEC with and without staining for the transcription factor Ctip2, marking neurons in LVb (magenta; scale bars are 500 μm). IL, infralimbic cortex; PER, perirhinal cortex; POR, postrhinal cortex.

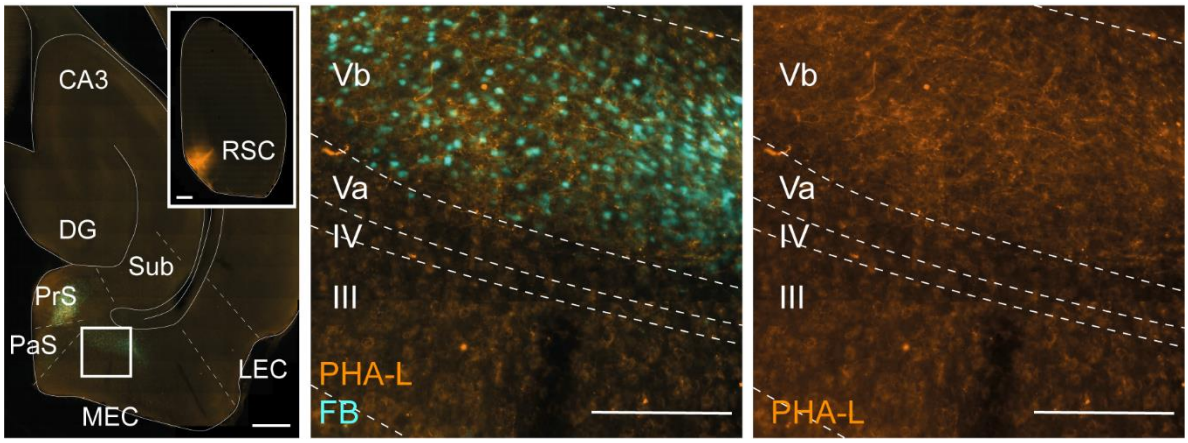

Figure S4. Inputs from retrosplenial cortex (RSC) to LV of MEC preferentially terminates in LVb.

Distribution of labeled fibers (orange) in MEC following a PHA-L injection into RSC (inset left-hand panel; scale bar equals 1000 μm; the experiment is the same as in Figure 3C). LVb neurons are retrogradely labeled with FB (cyan), which was injected into the superficial layers of MEC. The boxed area, indicated in the left hand panel is shown in the middle and right-hand panel with and without the retrogradely labeled LVb neurons, respectively (scale bars are 500 μm).

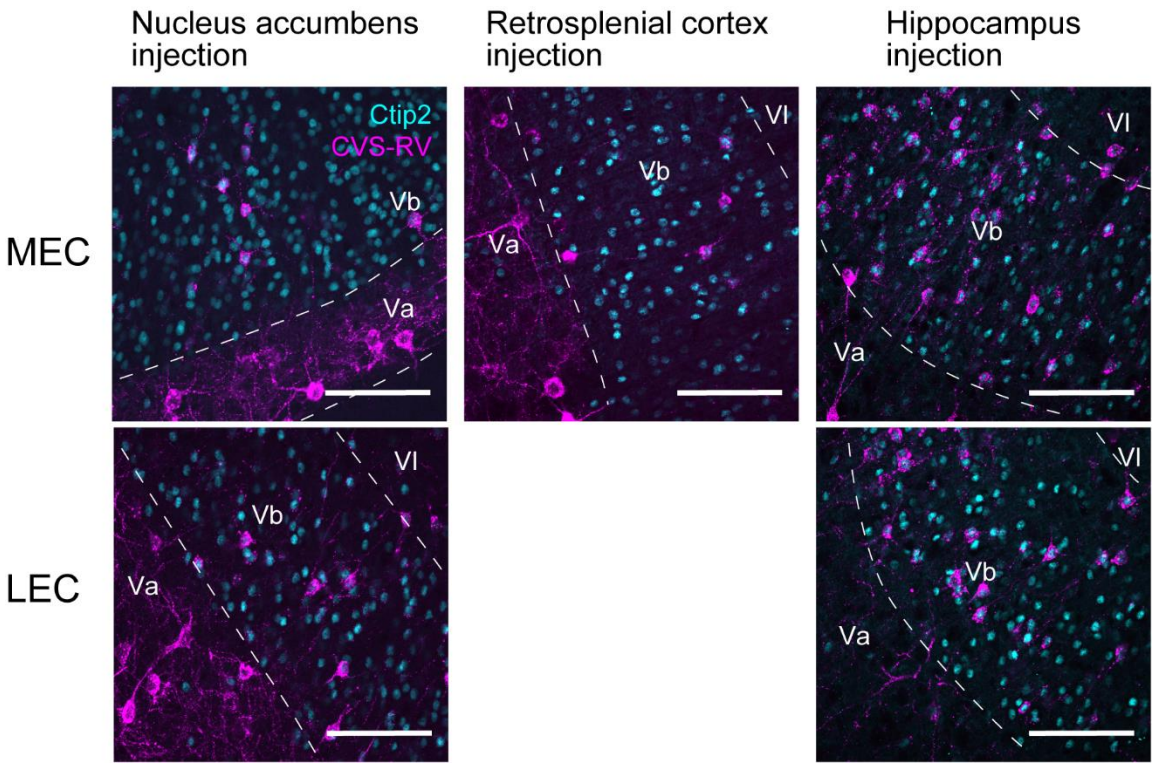

Figure S5. The majority of the transsynaptically labeled LVb neurons do express the transcription factor Ctip2.

Confocal images of neurons expressing CVS-RV (magenta) and Ctip2-labeled LVb neurons (cyan) after CVS-RV injection into the NAc (left-hand column), RSC (middle column) or the hippocampus (right-hand column). The majority of the CVS-RV-labeled neurons in LVb stain positive for Ctip2 as well. Scale bars are 100 μm.

Table S1. Number of EC labeled neurons after viral injection into the nucleus accumbens

A. Retrograde tracing with ΔG-RV (N=7)

Sample[1]	NAc-ΔG-1c		NAc-ΔG-2c		NAc-ΔG-3c		NAc-ΔG-4c		NAc-ΔG-5h		NAc-ΔG-6h		NAc-ΔG-7h	
	MEC	LEC	MEC	LEC	MEC	LEC	MEC	LEC	MEC	LEC	MEC	LEC	MEC	LEC
LII	2	20	0	1	1	3	2	13	5	17	1	5	4	6
LIII	6	49	0	5	1	14	0	7	5	31	6	20	0	10
LVa	65	298	1	55	17	122	3	45	122	343	82	253	38	191
LVb	8	47	0	3	0	9	1	2	4	14	0	10	1	3
LVI	2	10	0	0	0	3	0	6	7	17	1	3	0	3

B. Retrograde transsynaptic tracing with RV-CVS (N=4)

Sample[1]	NAc-CVS-1c		NAc-CVS-2c		NAc-CVS-3h		NAc-CVS-4h	
	MEC	LEC	MEC	LEC	MEC	LEC	MEC	LEC
LII	48	97	124	183	46	194	163	138
LIII	34	139	69	284	56	407	147	347
LVa	158	289	113	143	245	353	213	233
LVb	116	293	47	176	219	457	188	271
LVI	17	139	19	54	93	155	116	114

[1] The last character in the sample name shows how the sample was sectioned; c, coronal; h, horizontal.

Table S2. Number of EC labeled neurons after viral injection into the retrosplenial cortex

A. Retrograde tracing with ΔG-RV (N=4)

Sample[1]	RSC-ΔG-1s		RSC-ΔG-2s		RSC-ΔG-3s		RSC-ΔG-4c	
	MEC	LEC	MEC	LEC	MEC	LEC	MEC	LEC
LII	0	-	0	-	2	-	0	-
LIII	0	-	2	-	4	-	0	-
LVa	14	-	23	-	102	-	39	-
LVb	0	-	5	-	4	-	0	-
LVI	0	-	0	-	3	-	0	-

B. Retrograde transsynaptic tracing with RV-CVS (N=4)

Sample[1]	RSC-CVS-1s		RSC-CVS-2s		RSC-CVS-3c		RSC-CVS-4c	
	MEC	LEC	MEC	LEC	MEC	LEC	MEC	LEC
LII	89	-	346	-	23	-	31	-
LIII	142	-	460	-	21	-	47	-
LVa	147	-	415	-	103	-	212	-
LVb	85	-	378	-	130	-	132	-
LVI	32	-	118	-	14	-	0	-

[1] The last character in the sample name shows how the sample was sectioned; c, coronal; s, sagittal.

Table S3. Number of EC labeled neurons after viral injection into the hippocampus

A. Retrograde tracing with ΔG-RV (N=6)

Sample[1]	HIP-ΔG-1c		HIP-ΔG-2c		HIP-ΔG-3c		HIP-ΔG-4h		HIP-ΔG-5h		HIP-ΔG-6h	
	MEC	LEC	MEC	LEC	MEC	LEC	MEC	LEC	MEC	LEC	MEC	LEC
LII	22	304	12	356	1	25	186	212	44	125	46	89
LIII	43	84	2	41	1	12	335	13	520	219	124	45
LVa	1	0	0	3	0	0	4	1	0	0	2	3
LVb	0	1	0	0	0	0	0	0	1	0	1	0
LVI	0	1	0	2	0	0	5	2	0	1	3	0

B. Retrograde transsynaptic tracing with RV-CVS (N=4)

Sample[1]	HIP-CVS-1c		HIP-CVS-2c		HIP-CVS-3h		HIP-CVS-4h	
	MEC	LEC	MEC	LEC	MEC	LEC	MEC	LEC
LII	23	367	64	136	300	134	483	222
LIII	86	353	404	361	197	111	786	363
LVa	25	136	66	143	32	27	113	145
LVb	96	476	56	193	160	103	801	445
LVI	38	139	66	85	41	25	111	84

[1] The last character in the sample name shows how the sample was sectioned; c, coronal; h, horizontal.